

# Self-bound droplets of a dilute magnetic quantum liquid

Matthias Schmitt<sup>1</sup>, Matthias Wenzel<sup>1</sup>, Fabian Böttcher<sup>1</sup>, Igor Ferrier-Barbut<sup>1</sup> & Tilman Pfau<sup>1</sup>

<sup>1</sup>5. Physikalisches Institut und Center for Integrated Quantum Science and Technology, Universität Stuttgart, Pfaffenwaldring 57, 70550 Stuttgart, Germany

Self-bound many-body systems occur in different scenarios all across the fields of physics. For example in the astrophysical context the stellar classification is based on a detailed balance of attractive self-gravitating forces and repulsive terms e.g. due to Fermi pressure. Also liquid droplets are formed by mutual attractive forces due to covalent or van der Waals attraction and repulsive parts of the inter-particle potential due to the electronic Pauli exclusion principle. Self-bound ensembles of ultracold atoms at densities 100 million times lower than in a helium droplet, the only other quantum liquid known so far, have been suggested<sup>1,2</sup>. However, they have been elusive up to now as they require more than the usual contact interaction, which is either attractive or repulsive but never both. Based on the recent finding that an unstable bosonic dipolar gas can be stabilized by a repulsive many-body term<sup>3</sup>, which is due to quantum depletion and a corresponding exclusion volume at small distances, it was predicted that three dimensional self-bound quantum droplets of magnetic atoms should exist<sup>4,5</sup>. Here we report on their first observation in a trap-free levitation field. We find that this magnetic quantum liquid requires a minimum critical number of atoms below which it evaporates into an expanding gas due to the quantum pressure of the individual constituents.

While solitons are specific excited states where the underlying binding mechanism is based on an interplay of single-particle dispersion and two-body interaction<sup>6,7</sup>, self-bound droplets of a liquid are bound in their ground state and are formed due to a balance of attractive and repulsive forces of their constituents. Further examples are nuclei<sup>8</sup> which are based on a balance of an attractive short-range nuclear force and the Pauli and Coulomb repulsion of the nucleons. Also liquid droplets of water or helium are formed by mutual attractive forces and repulsive parts of the inter-particle potential. Especially helium droplets have opened up an intense field of research due to their interesting quantum nature<sup>9,10</sup>. Droplets can serve as closed isolated quantum systems for example to probe superfluidity of mesoscopic ensembles<sup>11</sup>. In the context of ultracold atoms, the observation of an ensemble of stable droplets<sup>12</sup> in a dilute magnetic quantum gas opened up the possibility for a three dimensional self-bound state<sup>4,5</sup>. A trapped quantum droplet of magnetic atoms has very recently also been observed using erbium atoms<sup>13</sup>. Here we demonstrate the first observation of self-bound liquid droplets in a sample of ultracold bosonic dysprosium atoms which have a strong long-range magnetic dipolar interaction and a tuneable repulsive short-range contact interaction. The interplay between these two interactions

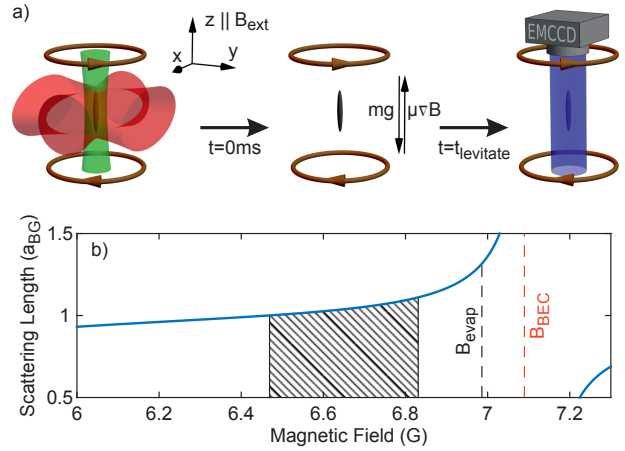


Figure 1: a) The experimental sequence as a schematic drawing: We start with an atomic ensemble in a crossed optical trap superimposed with a magnetic field gradient, strong enough to compensate the gravitational force. We turn off the trapping beams and levitate the droplet for various times  $t_{\text{levitate}}$ . We finally image the atoms using phase-contrast polarization imaging. b) Scattering length over magnetic field at the region of the Feshbach resonance in units of the positive background scattering length  $a_{\text{BG}}$ . The red dashed line indicates the field where we create a BEC. The hatched area describes the region where the experiments have been performed. The dashed black line shows the magnetic field used to intentionally evaporate the droplets to the gas phase.

can be tuned such that the overall mean field is weakly attractive but the interactions create quantum depletion and a corresponding many-body repulsion. The latter counteracts the attraction at a saturation density. At small atom numbers of  $\sim 1000$  atoms the finite size leads to a quantum pressure for every individual atom that results in an evaporation out of the selfbinding potential. Therefore these droplets are bound only above a critical atom number, which we investigate systematically.

We employ  $^{164}\text{Dy}$ , which possesses one of the strongest magnetic dipole moments in the periodic table with  $\mu = 9.93 \mu_B$  where  $\mu_B$  is the Bohr magneton. These atoms also offer control on the short-range interaction by a magnetic field using Feshbach resonances<sup>14–16</sup>. Here we use a specific resonance at a field of  $B_0 = 7.117(3)$  G with a width of  $\Delta B = 51(15)$  mG. This resonance allows tuning of the scattering length from a dipole-dominated sample to a contact-dominated sample without strong losses as shown in figure 1b). To quantify this we describe the interaction strengths using the relative dipolar strength  $\epsilon_{\text{dd}} = a_{\text{dd}}/a$  with the dipolar length  $a_{\text{dd}} = \mu_0 \mu^2 m / 12 \pi \hbar^2 \simeq 131 a_0$  where  $a_0$  is the Bohr radius,  $\hbar$  the reduced Planck constant,  $\mu_0$  the vacuum per-

meability and  $m$  the atomic mass. To observe the self-bound state, we shape an initially oblate Bose-Einstein condensate<sup>17</sup> of  $^{164}\text{Dy}$  at large scattering length ( $B_{\text{BEC}} = 7.089(5)$  G), where the interaction is contact-dominated, by an additional optical trap into a prolate shape along the magnetic field direction. This reshaping is done in two stages: first, we ramp a focussed beam at a wavelength of 532 nm aligned in the  $z$  direction within 50 ms. With this attractive potential the radial trap frequencies are increased to change the trap aspect ratio  $\lambda = \omega_z/\omega_\rho$  from 3.9 down to 1.5. Second, we apply a magnetic field gradient to the atomic cloud to levitate it by compensating the gravitational force. In this configuration, the cloud undergoes a continuous crossover from the BEC state directly into the single droplet ground state when lowering the scattering length, bypassing a bistable region<sup>4,18</sup>. In the consecutive 50 ms we lower the field to various values between  $B = 6.831(5) - 6.469(5)$  G, indicated in figure 1b) as hatched area, to lower the scattering length and create a single droplet. We hold the atoms in this configuration for 10 ms before ramping the optical trap powers within 20 ms to  $\approx 5\%$  of their initial values, keeping a constant trap aspect ratio. At this point we suddenly turn off the trap and image the cloud using far-detuned phase-contrast polarization imaging after various levitation times up to  $t_{\text{levitate}} = 90$  ms. This is schematically shown in figure 1a). Being sensitive only to high densities, we observe that a thermal fraction expands very quickly, while a very small and dense cloud remains for very long times. We interpret this as a self-bound quantum droplet. The size of the quantum droplets is smaller than our imaging resolution such that we observe astigmatic diffraction (see figure 2a)). At specific fields, we observe these droplets for times as long as  $t_{\text{levitate}} = 90$  ms. At some time during the trap-free levitation, we observe that the droplets have expanded. We interpret this behaviour by the fact that droplets lose atoms due to three-body decay or evaporation of excitations until they reach a critical atom number below which they are not self-bound anymore and evaporate back into a gas phase. Given our shot-to-shot noise in the initial atom number, this critical number is reached for various times. This behaviour is represented in figure 2a).

As a first analysis we count the images where we still observe a single droplet out of 100 shots and plot the survival probability for different magnetic fields in figure 2b) as histograms. The levitation time is changed between  $t_{\text{levitate}} = 0$  ms, which basically represents a trapped cloud, up to  $t_{\text{levitate}} = 90$  ms. We can see that for low scattering length ( $B = 6.469(5)$  G) we always create a single droplet but the lifetime is short. As the scattering length increases, the lifetime increases as well. We find a maximal survival probability for a magnetic field of  $B = 6.676(5)$  G. For even higher scattering lengths we only find droplets at 0 ms and very few self-bound droplets. These histograms are in qualitative agreement with an increasing critical atom number and decreasing atom loss rate in the droplets for increasing scattering length as was observed in reference<sup>3</sup> in a waveguide configuration. However the precise evolution is very dependent on the spread in initial atom number as well as fluctua-

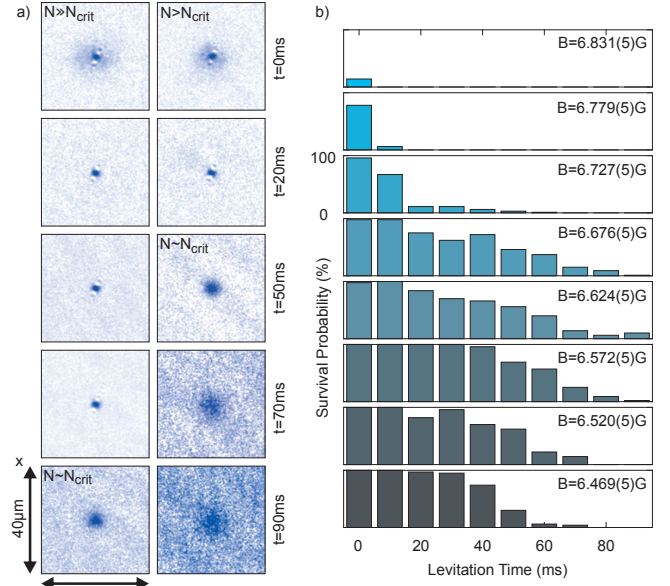


Figure 2: a) We show two traces of droplets for variable levitation times at the same magnetic field of  $B = 6.676(5)$  G. These images are not multiple images of the same droplet but rather selected from a variety of images as the imaging process is destructive. All images are rescaled to the maximum optical density. In the first column we start with an atom number much larger than the critical atom number for stable droplets and observe a single droplet up to  $t_{\text{levitate}} = 70$  ms. Between 70 - 90 ms the cloud reaches the critical atom number and evaporates back to a gas phase, observed as an expanding cloud. In the second column we show a droplet that starts with an atom number much closer to the critical atom number leading to an earlier evaporation, already between 20 - 50 ms of levitation time. From this point the cloud evaporates to the BEC phase and expands. b) Histogram of the surviving probability of a single droplet as function of levitation time and magnetic field. At low scattering length ( $B = 6.469(5)$  G) we always observe droplets for up to  $t_{\text{levitate}} = 30$  ms, followed by a fast decay which is explained by fast atom number decay due to three-body collisions. For increasing scattering length we observe an increase of the lifetime of these droplets up to a magnetic field of  $B = 6.676(5)$  G. At these conditions we observe a single droplet of a size below our resolution after a levitation time of  $t_{\text{levitate}} = 90$  ms. Further increase of the scattering length shows a fast decay of self-bound droplets already for short times ( $t_{\text{levitate}} = 20$  ms) which we interpret as originating from an increase of the critical atom number to values close to our initial atom number. For the highest scattering length ( $B = 6.831(5)$  G) we barely create droplets in the trap.

tions in the critical atom number.

To obtain a more quantitative analysis of the critical atom number of these droplets we intentionally evaporate them after variable levitation times by increasing the mag-

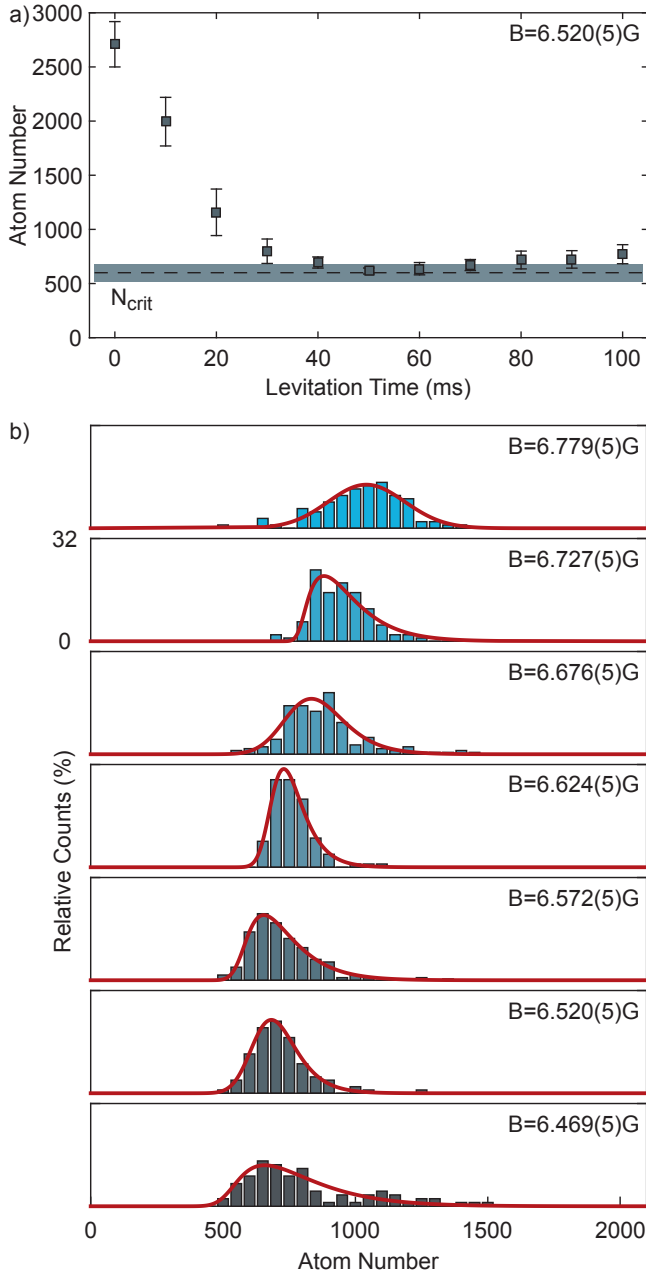


Figure 3: a) We show the atom number decay as function of levitation time. We observe a decay for short times to an essentially constant number for long times. The dashed line shows the critical atom number as best fit of our model (see text) to the data with the shaded area representing the error. b) We analyse the atom number distribution for levitation times in the range of  $t_{levitate} = 60 - 100$  ms since the atom number is mostly constant there. We bin the atom number to a window of 50 atoms and plot the relative counts as function of atom number and magnetic field. The red curve represents a fit of the convoluted function to the observed histograms. The color of the plotted histograms directly connects to the color shown in figure 2b) representing the magnetic field change.

netic field back to  $B_{evap} = 6.986(5)$  G shown as dashed black line in figure 1b). At this field the critical atom number is higher than all relevant atom numbers observed here. After expansion the atom number can be determined accurately without being limited by the finite resolution of the imaging optics. Here we observe that the number of atoms in the droplets decays to an essentially constant number, a further indication of a critical atom number for the self-bound droplets. This is shown in figure 3a) for a magnetic field of  $B = 6.520(5)$  G. Each point is represented by a mean atom number calculated from 20 images with the error denoting one standard deviation. A histogram of the atom number distribution for long levitation times ( $t_{levitate} \geq 60$  ms) for different magnetic fields is shown in figure 3b). We observe that the atom number distributions shift with scattering length and conclude that the droplets loose atoms until they reach the critical atom number, at which point they start evaporating to the gas phase. We observe that at long times, when most droplets have evaporated, there is an asymmetric dispersion in atom number. We posit that this reflects the fact that droplets do not evaporate all exactly at the same atom number, but the evaporation is a stochastic phenomenon. This can occur for some droplets with  $N > N_{crit}$  due to the presence of residual (e.g. thermal) excitation.

To extract a critical atom number we fit the histograms with a convolution of a Gaussian distribution, representing our statistical errors including detection noise, and a Maxwell-Boltzmann distribution, taking the finite evaporation rate at  $N > N_{crit}$  into account.

The best fits are shown in figure 3b) as red curves. We plot our result of the critical atom number in figure 4 and compare it to full Gross-Pitaevskii simulations<sup>19</sup>. The error is given by the quadratic mean of the width of the Maxwell-Boltzmann and Gaussian distribution. Note that this way of determining  $N_{crit}$  is dependent on the fit model and other definitions could lead to slightly different values. Nevertheless, we can see a clear change of the critical atom number with magnetic field and with this we probe the phase transition line between the liquid phase and the gas phase. To compare the results with the simulations we calculate the relative dipolar strength for our magnetic field range. To do so we include the Feshbach resonance at  $B_{01} = 7.117(3)$  G with a width of  $\Delta B_1 = 51(15)$  mG as well as a resonance at  $B_{02} = 5.1(1)$  G with a width of  $\Delta B_2 = 0.1(1)$  G. A best fit is obtained when we change the previously assumed local background scattering length<sup>15</sup> from  $a_{bg} = 92(8) a_0$  to  $a_{bg} = 62.5 a_0$ . Although this value exceeds the respective error bounds we find that this new value agrees with earlier publications comparing theory<sup>18,20</sup> and experiments<sup>3,12</sup>. This change impacts the critical atom number by a factor 10, and despite our model-dependent estimation, this measurement gives precise bounds on the local background scattering length. Given the large density of resonances it is possible that the local background scattering length in this magnetic field range can be different from the one measured at

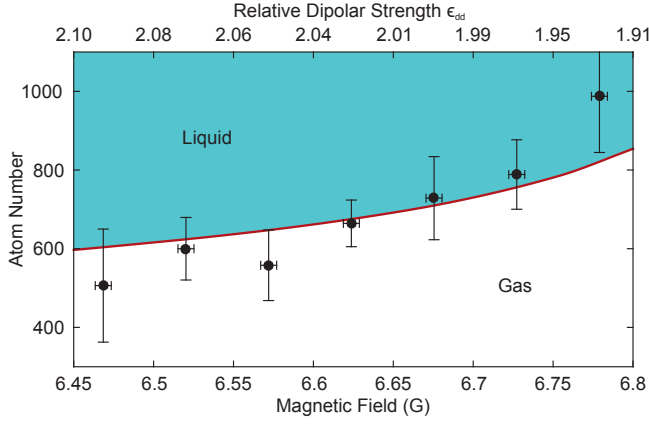


Figure 4: Critical atom number as a function of the magnetic field taking the fit values from figure 3b). The error in the atom number is given by the quadratic mean of  $\sigma$  and  $\Delta N$  while the error in magnetic field describes the resolution of our magnetic field coils. For decreasing magnetic field the critical atom number  $N_{crit}$  decreases as well. We identify the upper left corner as the liquid phase and the lower right corner as the gas phase. Here the critical atom number describes the measure of the phase transition between liquid and gas. The solid red line represents a full Gross-Pitaevskii simulation for different relative dipolar strengths  $\epsilon_{dd}$ .

$B = 1.581(5)$  G earlier<sup>15</sup>. Note however that there is currently no independent absolute scattering length measurement at this magnetic field. Therefore the agreement between theory and experiment is subject to independent confirmation.

This observation of quantum droplets of a liquid at densities 100 million times lower than helium droplets being the only other previously known quantum liquid, opens up a new field in ultracold atoms. It provides a truly closed quantum system since it is completely decoupled from any laser fields. Our discovery can strongly reinforce the connection between the field of Bose-Einstein condensates and helium nano droplets<sup>21</sup>, for instance through the measurement of collective excitations which have been calculated in that context<sup>22</sup>.

## Methods

**Gross-Pitaevskii simulation** In order to compare our results to the current theory<sup>4,5</sup> we perform simulations of the effective Gross-Pitaevskii equation

$$i\hbar\partial_t\psi = \left[ -\frac{\hbar^2\nabla^2}{2m} + V_{ext} + g|\psi|^2 + \int d\mathbf{r}' V_{dd}(\mathbf{r} - \mathbf{r}')|\psi(\mathbf{r}')|^2 + \frac{32g\sqrt{a^3}}{3\sqrt{\pi}}\left(1 + \frac{3}{2}\epsilon_{dd}^2\right)|\psi|^3 - i\frac{\hbar}{2}L_3|\psi|^4 \right]\psi(\mathbf{r}) \quad (1)$$

taking into account quantum fluctuations within a local density approximation<sup>23,24</sup> and three-body losses. The validity of the local density approximation was confirmed by quantum Monte Carlo simulations in reference<sup>25</sup> as well as recent measurements with erbium atoms<sup>13</sup>. The dipolar and scattering lengths are  $a_{dd} = 131 a_0$  and  $a = 62 - 70 a_0$ . The latter defines  $g = 4\pi\hbar^2/m$  and is chosen such that we are in agreement with the critical atom numbers we observe in the experiment. The loss parameter  $L_3 = 1.25 \cdot 10^{-41} \text{ m}^6/\text{s}$  is estimated from measurements on a thermal cloud and is assumed to be constant over the small range of scattering length.

To obtain the data in figure 4 we choose  $V_{ext} = 0$  and initially prepare  $N_0 > N_{crit}$  atoms with a gaussian density distribution ( $\sigma_r = 250 \text{ nm}$ ,  $\sigma_z = 1500 \text{ nm}$ ). The ground state is reached by imaginary time evolution of equation (1) with a split-step Fourier method. Following this preparation of the self-bound droplet with  $N_0$  atoms we simulate the dynamics via real-time evolution. Since the atom number  $N < N_0$  decays due to three-body losses, the density and the effective two-body attraction are reduced as well. At  $N = N_{crit}$  the contributions by the effective two-body attraction and the quantum pressure are the same in magnitude and the droplet evaporates quickly. This evaporation process manifests itself by a drop in peak density of at least one order of magnitude. Three-body losses are highly suppressed then, such that the atom number stays almost constant for an evaporated droplet.

1. Petrov, D. S. Quantum mechanical stabilization of a collapsing Bose-Bose mixture. *Phys. Rev. Lett.* **115**, 155302 (2015).
2. Bulgac, A. Dilute quantum droplets. *Phys. Rev. Lett.* **89**, 050402 (2002).
3. Ferrier-Barbut, I., Kadau, H., Schmitt, M., Wenzel, M. & Pfau, T. Observation of quantum droplets in a strongly dipolar Bose gas. *Phys. Rev. Lett.* **116**, 215301 (2016).
4. Wächtler, F. & Santos, L. Ground-state properties and elementary excitations of quantum droplets in dipolar Bose-Einstein condensates. *arXiv:1605.08676* (2016).
5. Baillie, D., Wilson, R. M., Bisset, R. N. & Blakie, P. B. Self-bound dipolar droplet: a localized matter-wave in free space. *arXiv:1606.00824* (2016).
6. Strecker, K. E., Partridge, G. B., Truscott, A. G. & Hulet, R. G. Formation and propagation of matter-wave soliton trains. *Nature* **417**, 150–153 (2002).
7. Khaykovich, L. *et al.* Formation of a matter-wave bright soliton. *Science* **296**, 1290–1293 (2002).
8. Bender, M., Heenen, P.-H. & Reinhard, P.-G. Self-consistent mean-field models for nuclear structure. *Rev. Mod. Phys.* **75**, 121–180 (2003).
9. Volovik, G. *The Universe in a Helium Droplet* (Oxford Science Publications, 2009).



10. Toennies, J. P. & Vilesov, A. F. Superfluid helium droplets: A uniquely cold nanomatrix for molecules and molecular complexes. *Angewandte Chemie International Edition* **43**, 2622–2648 (2004).
11. Gomez, L. F. *et al.* Shapes and vorticities of superfluid helium nanodroplets. *Science* **345**, 906–909 (2014).
12. Kadau, H. *et al.* Observing the Rosensweig instability of a quantum ferrofluid. *Nature* **530**, 194–197 (2016).
13. Chomaz, L. *et al.* Quantum-fluctuation-driven crossover from a dilute Bose-Einstein condensate to a macrodroplet in a dipolar quantum fluid. *arXiv:1607.06613* (2016).
14. Chin, C., Grimm, R., Julienne, P. & Tiesinga, E. Feshbach resonances in ultracold gases. *Rev. Mod. Phys.* **82**, 1225–1286 (2010).
15. Tang, Y., Sykes, A., Burdick, N. Q., Bohn, J. L. & Lev, B. L. *s*-wave scattering lengths of the strongly dipolar bosons  $^{162}\text{Dy}$  and  $^{164}\text{Dy}$ . *Phys. Rev. A* **92**, 022703 (2015).
16. Maier, T. *et al.* Emergence of chaotic scattering in ultracold Er and Dy. *Phys. Rev. X* **5**, 041029 (2015).
17. Lu, M., Burdick, N. Q., Youn, S. H. & Lev, B. L. Strongly dipolar Bose-Einstein condensate of dysprosium. *Phys. Rev. Lett.* **107**, 190401 (2011).
18. Bisset, R. N., Wilson, R. M., Baillie, D. & Blakie, P. B. Ground state phase diagram of a dipolar condensate with quantum fluctuations. *arXiv:1605.04964* (2016).
19. See Methods section.
20. Wächtler, F. & Santos, L. Quantum filaments in dipolar Bose-Einstein condensates. *Phys. Rev. A* **93**, 061603 (2016).
21. Dalfó, F. & Stringari, S. Helium nanodroplets and trapped Bose-Einstein condensates as prototypes of finite quantum fluids. *The Journal of Chemical Physics* **115**, 10078–10089 (2001).
22. Casas, M. & Stringari, S. Elementary excitations of  $^4\text{He}$  clusters. *Journal of Low Temperature Physics* **79**, 135–149 (1990).
23. Lima, A. R. P. & Pelster, A. Quantum fluctuations in dipolar Bose gases. *Phys. Rev. A* **84**, 041604 (2011).
24. Lima, A. R. P. & Pelster, A. Beyond mean-field low-lying excitations of dipolar Bose gases. *Phys. Rev. A* **86**, 063609 (2012).
25. Saito, H. Path-integral Monte Carlo study on a droplet of a dipolar Bose-Einstein condensate stabilized by quantum fluctuation. *Journal of the Physical Society of Japan* **85**, 053001 (2016).

**Acknowledgements** We thank H. P. Büchler, L. Santos, F. Ferlaino, W. Ketterle, H. Sadeghpour, M. Zwerlein and V. Vuletić for discussions. This work is supported by the German Research Foundation (DFG) within SFB/TRR21 as well as FOR 2247. I.F.B. acknowledges support from the EU within Horizon2020 Marie Skłodowska Curie IF (703419 DipInQuantum).